Measurement of noise exposure planar distribution in aircraft approach path vicinity

Hirokazu ISHII[1]; Takatoshi YOKOTA[2]; Koichi MAKINO[3];
Naoaki SHINOHARA[4]; Masayuki SUGAWARA[5]

[1] Japan Aerospace Exploration Agency, Japan

[2, 3] Kobayasi Institute of Physical Research, Japan

[4] Narita International Airport Promotion Foundation, Japan

[5] Airport Environment Improvement Foundation, Japan

ABSTRACT

Japan Aerospace Exploration Agency is conducting a research project called DREAMS which aims to develop key technologies for future air traffic management systems which will enhance safety, efficiency, user convenience and environmental compatibility of flight operations. One of the research subjects in DREAMS is noise abatement flight technology. Its key element is an aircraft noise prediction model taking into account the effect of meteorological conditions on noise propagation. In order to verify the developed noise prediction model, noise measurement was conducted to obtain the planar distribution of noise exposure below the approach paths. The measurement area was about 4- by 4.4-kilometers and was divided into 110 (11×10) 400- by 400-meter grids. A GPS-synchronized multipoint noise measurement system was placed in every grid. The obtained results proved that the predicted instantaneous noise level and the noise exposure level were in good agreement with the measurement. The average and standard deviation of the noise exposure level prediction error calculated from 2543 data for Boeing 777-300ER were 0.41 dB and 1.50 dB, respectively.

Keywords: Aircraft Noise, Measurement, Prediction   I-INCE Classification of Subjects Number(s): 76.1.3

1. INTRODUCTION

Demand for world air transportation is forecast to grow around 2.5±0.3 times over the next 20 years (1). Since this volume of air traffic is already approaching and will soon exceed the capacity limit posed by the current air traffic control, there is a need for new air traffic management (ATM) system capable of enhancing the safety and improving the efficiency and environmental compatibility of air transportation.

The International Civil Aviation Organization (ICAO) has introduced a Global ATM Operational Concept (2). It presents a vision of an integrated, harmonized and globally interoperable ATM system, and describes a comprehensive concept of a global integrated ATM system based on clearly established operational requirements. ICAO has also published Global Air Navigation Plan (3), which serves as a strategic document providing the methodology for global air navigation harmonization. Considerable efforts to implement next generation ATM systems are being made by NextGen in the United States (4) and SESAR (Single European Sky ATM Research) in Europe (5).

Air traffic in Japan is also forecast to grow 1.5 times over the period 2005-2027. The Japan Civil Aviation Bureau has established a long-term plan called CARATS (Collaborative Actions for

[1] ishii.hirokazu@jaxa.jp
[2] t-yokota@kobayasi-riken.or.jp
[3] makino@kobayasi-riken.or.jp
[4] shino@napf.or.jp
[5] m-sugawara@center.aeif.or.jp

Renovation of Air Traffic System) (6) and has initiated collaborative work among industry, academia and government to reform Japan's ATM system.

The Japan Aerospace Exploration Agency (JAXA) is engaged in the development of future ATM systems under a research project called DREAMS (Distributed and Revolutionarily Efficient Air-traffic Management System) (7). One of the research subjects in DREAMS is noise abatement flight technology. It aims to maintain community noise exposure at current levels even in the presence of up to a 50 percent increase in traffic volume. In order to achieve this goal, JAXA is currently developing a system that optimizes approach paths taking account of the meteorological effects on noise propagation. A key element of the system is the development of an appropriate noise model, which can compute a time series of instantaneous noise levels at arbitrary observer positions taking into account the effect of meteorological conditions on noise propagation.

This paper first gives an overview of the noise prediction models. Then it outlines a series of experiments to obtain planar distribution of noise exposure around approach paths. The measured and the predicted noise exposure are compared to verify the accuracy of the model.

2. Overview of Noise Prediction Model

In DREAMS' noise prediction model (8), instantaneous sound pressure level in arbitrary observer position was formulated as follows:

$$L_p^f(r) = L_w^f + \Delta L_{dir}^f - 11 - 20\log_{10}(r) + \Delta L_{grnd\&met}^f + \Delta L_{atm}^f \tag{1}$$

where

f	: octave band center frequency [Hz]
r	: distance between the source and observer [m]
$L_p^f(r)$	: sound pressure level at the observer [dB]
L_w^f	: sound power level of the source [dB]
ΔL_{dir}^f	: adjustment for three-dimensional directivity of the source [dB]
$\Delta L_{grnd\&met}^f$	: adjustment for the effects of ground and meteorological conditions [dB]
ΔL_{atm}^f	: adjustment for atmospheric attenuation [dB] (9)

The source model was defined as octave band sound power level, L_w^f, with adjustment of the three-dimensional directivity of the source, ΔL_{dir}^f, at given engine power setting. Both terms were developed from measured noise data (10). Figure 1 shows an example of the source model of Boeing 777-300ER (B77W) with twin GE90 turbofan engines during approach at corrected net thrust of 12,000 pound. The frequency characteristics and the longitudinal directivity were derived from the experimental results in this study. The Noise-Power-Distance data (11) for Boeing 777-200ER (B772) with the same GE90 engines was used to relate the sound power level at source, L_w^f, with corrected net thrust. Adjustment of lateral directivity was added according to reference (12) to obtain the three-dimensional directivity.

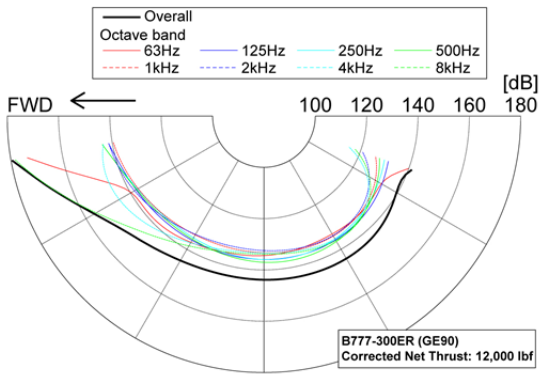

Figure 1 – An example of the source model in the longitudinal plane

The propagation model included spherical attenuation, atmospheric attenuation, and adjustment for the effect of ground and meteorological conditions as shown in Eq. (1). This study used two methods to obtain the meteorological effects on propagation, namely a numerical computation using

Green's Function Parabolic Equation (GF-PE) method for precise prediction and a table lookup for faster calculation.

Meteorological conditions in this study were considered in the view of wind and stability based on the classification proposed by HARMONOISE project (13), and typical speed of sound profiles were defined for all combination of the wind and the stability classes by using the speed of sound profile proposed by IMAGINE project (13). The GF-PE computations were then conducted with typical speed of sound profiles. The effects of atmospheric turbulence were also considered in the GF-PE computation by using von Karman distribution.

Figure 2 shows an example of the effects of ground and meteorological conditions, $\Delta L^{f}_{grnd\&met}$, prepared based on the GF-PE results and used in the table lookup. Note the ordinate of Figure 2(b) represents the altitude of the source, or aircraft. Since GF-PE computation is not valid above the elevation angle of 75 degree from the observer to the source (dashed lines in the Figure 2(b)) (14), GF-PE results in the regions were substituted by analytical results of ground effects of reflection and absorption.

As for aircraft noise prediction, a speed of sound profile was computed from the actual meteorological conditions, and one of the GF-PE results was picked up by choosing the typical speed of sound profile which maximized the coefficient of determination calculated for altitude from 0 to 650 m. Experimental studies to verify accuracy of these methods can be found in reference (15,16).

Ground surface	Grass	Wind class		2	Stability class		1	
Angle between propagation and wind direction [deg]				180	Oct. band Freq. [Hz]		500	

Unit: [dB]	Horizontal Distance from source to observer [m]								
Source Altitude [m]	61	121.9	192	304.8	609.6	1219.2	1920.2	3048	4876.8
2.5	−7.65	−15.56	−21.64	−24.2	−24.76	−22.89	−21.83	−22.13	−20.17
18.9	2.53	0.07	−1.88	−7.73	−22	−20.77	−19.57	−18.49	−18.78
41.5	1.28	2.06	2.15	−0.12	−10.33	−19.66	−17.75	−17.22	−17.81
68.3	2.21	1.09	1.89	2.14	−1.67	−13.87	−18.96	−18.13	−17.71
102.1	1.92	2.98	1.26	2.02	−0.15	−10.4	−14.59	−16.32	−16.2
147.5	1.63	2.17	2.23	1.51	2.8	−1.69	−13.86	−16.73	−15.23
214.9	1.85	1.9	2.22	1.31	1.82	0.74	−6.31	−12.16	−14.87
334.9	2.21	1.9	1.9	2.45	1.26	3.54	−0.81	−11.53	−13.6
609.6	2.38	2.18	1.64	1.63	2.61	2.14	3.54	−0.54	−7.15
1289.6	2.44	2.4	2.31	2.08	2.1	2.47	0.52	2.06	1.81

(a) Table of adjustment values

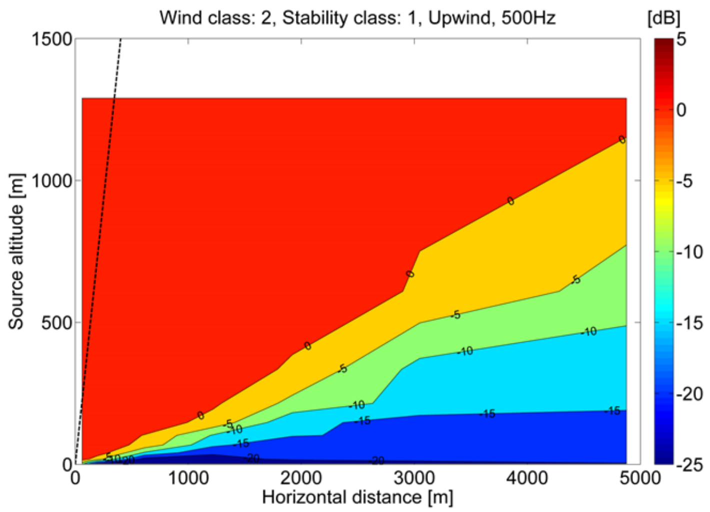

(b) Contour plot

Figure 2 – An example of effects of ground and meteorological conditions used in the table lookup

3. Noise Measurement Methods

3.1 Overview

A series of field experiments was carried out to obtain planar distribution of noise exposure around approach paths. This particular measurement area was selected considering terrain flatness, background noise, number of flights, and availability of measurement points.

Figure 3 shows the layout of the experimental field. It lies at 8-12 km south away from the runway 34R threshold at the Narita International Airport. The 4.4- by 4-km measurement area was divided into 110 (11×10) 400- by 400-meter grids. A measurement point was selected carefully within each grid considering accessibility and from the background noise by road traffic. Figure 3 also shows the elevation of the area relative to that of the runway 34R threshold. It is based on the digital elevation data published by Geospatial Information Authority of Japan. The measurement area can be approximated to flat surface without adding a significant error to the measurements.

3.2 Apparatus

Figure 4 and Table 1 show the noise measurement system used in this experiment (17). It consisted of a sound level meter, a recorder, and a GPS pulse generator.

The microphone of the sound level meter was set at 1.2-meter height with an all-weather windscreen. The rest of the system was contained in a closed box to avoid damage by rain as well as undesirable access to the system.

The GPS pulse generator emits periodical pulses at two different cycles, i.e. every 10 and 60 seconds. Sound pressure signal from the sound level meter and the GPS pulse were input separately into left and right channels of the recorder, respectively. These signals were recorded at sampling frequency of 22.05kHz and 16-bit quantization. All the noise data from 110 measurement points were synchronized using GPS pulses.

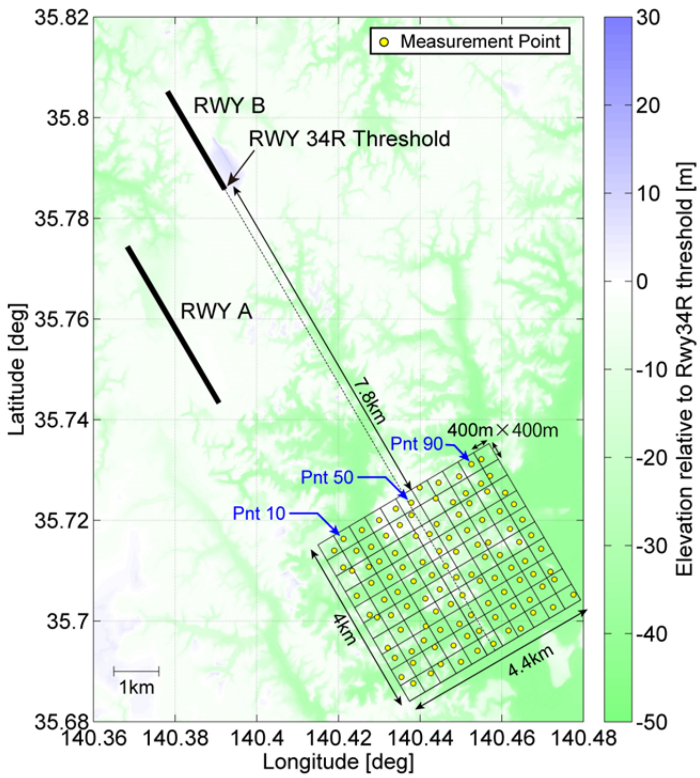

Figure 3 – Experimental field layout

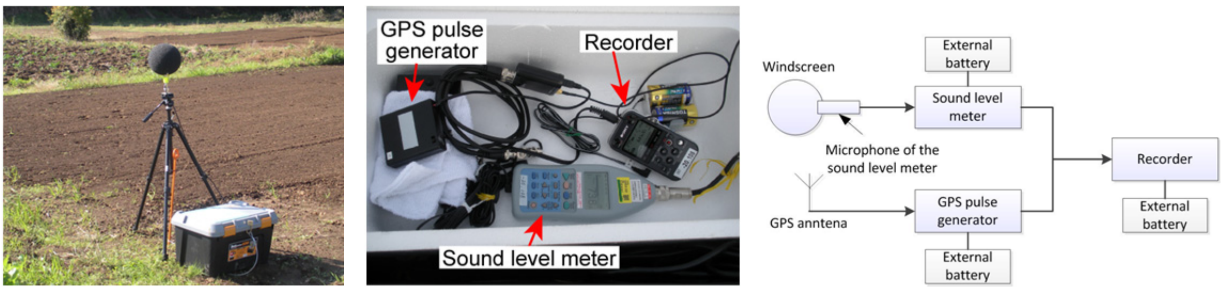

(a) Overview (b) Equipment in the box (c) Wiring diagram

Figure 4 – Noise measurement system

Table 1 – Components of the noise measurement system

Item	Manufacturer/Model
Sound level meter	Rion/NL-21
Windscreen	Rion/WS-03E
Recorder	SONY/M10
GPS pulse generator	u-blox/EVK$_{sc}$6T

4. Results and Discussion

The experiment presented in this paper was carried out on 13-22 November 2013. Table 2 shows the number of flights where measurement was successfully conducted. Note they are not the numbers of all flights approached to the airport, but those of target aircraft types operated by an airline that provided flight data for this research.

Octave band analysis was applied to the measured sound pressure and time series of A-weighted sound pressure level, L_A, was calculated. Single event noise exposure level (SEL), L_{AE}, was obtained by integrating L_A over the period of time while L_A was above $L_{A,max}$-10dB.

Predicted noise levels, L_A and L_{AE}, were computed using flight data from onboard Quick Access Recorders (QAR) and three-dimensional weather data. The weather data was obtained by numerical analysis using CReSS (Cloud Resolving Storm Simulator) model with Meso-Scale Model and sea surface temperature as initial and boundary conditions (18).

Table 2 – Number of measured and predicted flight (target aircraft type only)

Aircraft type	Boeing 777-300ER (B77W)	Boeing 777-200ER (B772)	Boeing 787-8 (B788)	Boeing 767-300ER (B763)
Number of flight measured	24	13	24	43

4.1 Time Series of Noise Level

Figure 5 shows time series of noise levels introduced by B77W and measured at points 10, 50, and 90 as shown in Figure 3. Table 3 shows the weather condition provided by the airport at the time of measurement.

A source noise measurement system (10) was placed at measurement point 50 independently of the noise measurement system described above. The power level at the source used in the source model was converted from the $L_{A,max}$ obtained by the source noise measurement system at point 50 by compensating for the spherical and the atmospheric attenuation.

The results presented in Figure 5 show clearly that the predicted noise levels are in good agreement with the measured results. It is therefore concluded that the noise prediction model developed in this study can predict instantaneous noise level introduced by aircraft noise accurately by considering meteorological effects on propagation.

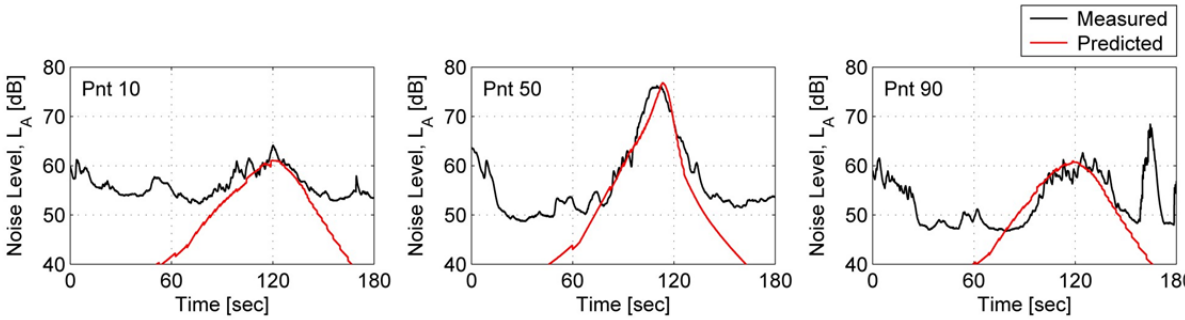

Figure 5 –Time series of noise levels

Table 3 – Weather conditions

Initial time	Wind direction	Wind speed	Temperature	Humidity
11/15 16:26:50	330 [deg]	2.6 [m/s]	9 [°C]	93 [%]

4.2 Noise Exposure Level

Figure 6 shows the distribution of noise exposure levels, L_{AE}, calculated from time series of noise levels, L_A, at the case shown in the previous section. Although there is small difference in the noise exposure level at each point, a common distribution pattern is observed.

Figure 7 shows the histogram of noise exposure level prediction error for B77W through the measurement. The data set consisted of 2543 measurement values after excluding invalid results from 2640 (24 flights × 110 points) measured data. The average and the standard deviation (S.D.) of the prediction error were 0.41 dB and 1.50 dB, respectively. It can be considered the prediction error (overestimation) was due to an error in the source model, because only the spherical and the atmospheric attenuation were compensated for as described above and the effect of sound reflection on the ground remained as the power level at the source. On the other hand, the adjustment for the effects of ground and meteorological conditions computed by GF-PE also includes the effects of sound reflection, thus it was double counted in the predicted noise levels. Although there was a small overestimation, it can be concluded that the noise prediction model developed in this study predicted noise exposure levels accurately.

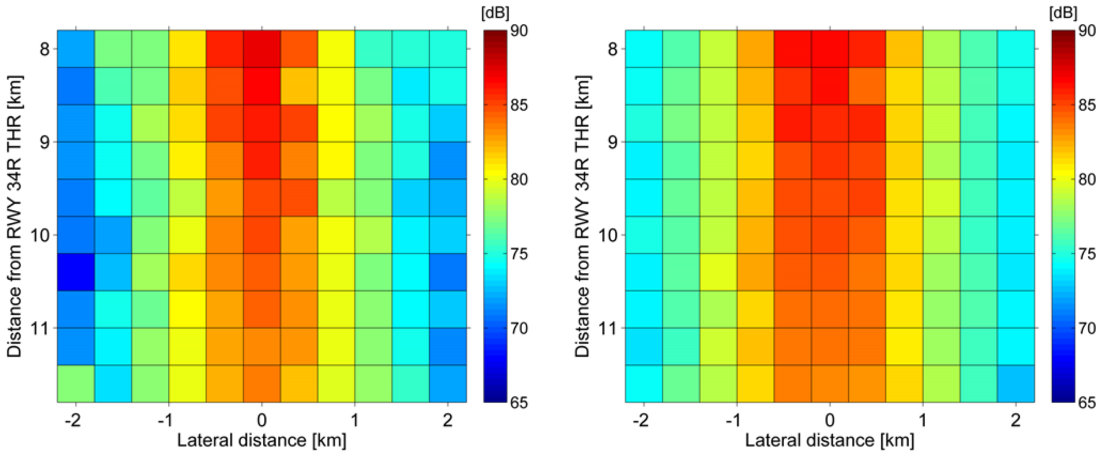

(a) Measured L_{AE} (b) Predicted L_{AE}

Figure 6 – Distribution of noise exposure level

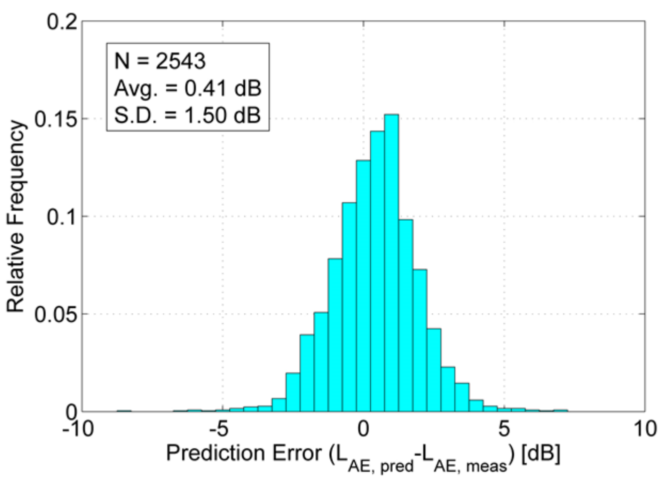

Figure 7 – Histogram of noise exposure level prediction error for B77W

5. Concluding Remarks

This paper presented the noise prediction model developed under JAXA's DREAMS project and a field experiment to measure the planar distribution of noise exposure. As a result, both predicted instantaneous noise level, L_A, and noise exposure level, L_{AE}, showed very good agreement with measured results. The prediction error of L_{AE} was quantitatively investigated, and the average and the standard deviation for Boeing B777-300ER were 0.41 dB and 1.50 dB, respectively.

The same experiments was carried out in spring 2014, and similar experiments with measurement points reduced to 10 representing points in winter and summer after the one presented in this paper. The obtained data are currently under analysis, and the results will be presented in the near future with further investigation of prediction accuracy and the improvement in the noise prediction model.

REFERENCES

1. ICAO Environmental Report 2013: Aviation and Climate Change. International Civil Aviation Organization; 2013.
2. Global air traffic management operational concept (Doc 9854). International Civil Aviation Organization; 2005.
3. Global air navigation plan (Doc 9750). 3rd ed. International Civil Aviation Organization; 2007.
4. NextGeneration Air Transport System (NextGen) [Internet]. Federal Aviation Administration; Available from: http://www.faa.gov/nextgen/
5. Research & SESAR [Internet]. EUROCONTROL; Available from: http://www.eurocontrol.int/sesar-research
6. Long-term vision for the future air traffic systems: Changes to intelligent air traffic systems [Internet]. 2010. Available from: http://www.mlit.go.jp/common/000128185.pdf
7. Ishii H, Okuno Y, Okada S, Ishikawa T, Yokota T, Sugawara M. JAXA's research plan for next generation air traffic management system (DREAMS) and noise abatement flight technologies. Proc INTER-NOISE 2012. 2012. p. 6108–15.
8. Ishii H, Harada K, Makino K, Yokota T, Shinohara N, Sugawara M. Development of an aircraft noise prediction model considering the effect of meteorological conditions in JAXA's DREAMS project. Proc INTER-NOISE 2013. Innsbruck, Austria; 2013.
9. Acoustics -- Attenuation of sound during propagation outdoors -- Part 1: Calculation of the absorption of sound by the atmosphere. ISO; 1993. Report No.: 9613-1.
10. Makino K, Yokota T, Okubo T, Matsumoto T, Yamamoto K, Kawase Y, et al. Development of the precise aircraft sound source model based on direction-of-arrival estimaton using cross-correlation technique. Proc INTER-NOISE 2013. Innsbruck, Austria; 2013.
11. Aircraft Noise and Performance Database [Internet]. EUROCONTROL; Available from: http://www.aircraftnoisemodel.org/
12. Method for Predicting Lateral Attenuation of Airplane Noise. SAE International; 2012. Report No.: SAE AIR 5662.
13. De Roo F, Salomons E, Heimann D, Hullah P. IMAGINE – Reference and Engineering Models for Aircraft Noise Sources, Volume 1. 2007. Report No.: IMA4DR-070323-EEC-10.
14. Gilbert KE, Di X. An exact point source starting field for the Fourier parabolic equation in outdoor sound propagation. J Acoust Soc Am. 2007;121(5):EL203–EL210.
15. Yokota T, Okubo T, Makino K, Matsumoto T, Yamamoto K, Ishii H, et al. Experimental study of meteorological effects on sound propagation from an elevated source. Proc INTER-NOISE 2013. Innsbruck, Austria; 2013.
16. Yokota T, Makino K, Matsumoto T, Yamamoto K, Ishii H. Experimental study of meteorological and ground effects on outdoor sound propagation for developing aircraft noise prediction model. Proc INTER-NOISE 2014. Melbourne, Australia; 2014.
17. Yokota T, Okubo T, Makino K, Matsumoto T, Yamamoto K, Ishii H, et al. Visualization of meteorological effects on aircraft noise propagation based on GPS-synchronized multipoint measurement. Proc INTER-NOISE 2012. 2012.
18. Yoshikawa E, Matayoshi N. Wake vortex observation campaign by ultra fast-scanning lidar in Narita airport, Japan. Proc ICAS 2014. St. Petersburg, Russia; 2014.